



# Prediction of three-body $B^0 \rightarrow \rho^- p \bar{n}$ , $\pi^- p \bar{n}$ decay rates

Chun-Kiang Chua, Wei-Shu Hou, Shang-Yuu Tsai

Department of Physics, National Taiwan University, Taipei, 10764 Taiwan, ROC

Received 8 August 2001; received in revised form 14 September 2001; accepted 17 September 2001

Editor: T. Yanagida

## Abstract

We predict the rates of the charmless three-body  $B^0 \rightarrow \rho^- p \bar{n}$  and  $\pi^- p \bar{n}$  modes due to weak vector current contributions to be  $\sim 4 \times 10^{-6}$  and  $2 \times 10^{-6}$ , respectively. The basis is a factorization approach of current produced nucleon pairs, together with an isospin transformation that relates nucleon weak vector form factors to electromagnetic form factors. Adding the axial vector current contribution, we find  $B^0 \rightarrow \rho^- p \bar{n}$  and  $B^+ \rightarrow \rho^0 p \bar{n}$  to be at  $10^{-5}$  order. The three-body modes appear to dominate over the two-body modes such as  $B \rightarrow p \bar{p}$ ,  $p \bar{\Lambda}$ .

© 2002 Elsevier Science B.V. Open access under [CC BY license](https://creativecommons.org/licenses/by/4.0/).

PACS: 13.25.Hw; 13.40.Gp; 14.20.Dh

## 1. Introduction

A large number of charmless mesonic decays of the  $B$  mesons have emerged since 1997, and are of great current interest. For example,  $\pi^+ \pi^- / K^+ \pi^- \sim 1/4 - 1/5$  suggests [1] that  $\phi_3$  (or  $\gamma$ )  $\equiv \arg V_{ub}^*$  could be  $90^\circ$  or more. A natural question to ask [2] is: what about charmless baryonic decays? The CLEO Collaboration has done some search in the past, but turning up null results for modes like  $B^0 \rightarrow p \bar{p}$  that are below the  $10^{-5}$  level [3]. The Belle Collaboration has recently improved the limits [4] on  $B^0 \rightarrow p \bar{p}$  by an order of magnitude, pushing down to the  $10^{-6}$  level. It is of interest to ask, therefore, if all charmless baryonic modes are below  $10^{-5}$ . In this Letter, from a suitably sound theoretical basis involving nucleon form factor

data, we show that  $B^0 \rightarrow \rho^- p \bar{n}$  could be a leading charmless baryonic decay with rate at the  $10^{-5}$  level.

The CLEO Collaboration recently reported the observation of the  $B^0 \rightarrow D^{*-} p \bar{n}$  mode at the  $10^{-3}$  level [5], which is only a factor of 4–5 lower than  $B^0 \rightarrow D^{*-} \rho^+$  and  $D^{*-} \pi^+$  [6]. Scaling by  $|V_{ub}/V_{cb}|^2$  one could already infer that  $B^0 \rightarrow \rho^- p \bar{n} \sim 10^{-5}$ , but a better understanding is desirable. A factorization approach for  $B^0 \rightarrow D^{*-} p \bar{n}$  with current produced nucleon pairs has been proposed recently [7]. The three-body decay is seen as generated by two weak currents: one converting  $B^0$  to  $D^{*-}$ , the other creating the nucleon pair. The nucleon weak vector form factors are related by isospin rotation to nucleon electromagnetic form factors. By using  $G_M^{p,n}$  measured from  $e^+ e^- \rightarrow \bar{N} N$  and  $p \bar{p} \rightarrow e^+ e^-$  processes [8–11], we are able to account for up to 60% of the observed rate, the remainder seemingly coming from axial vector current contribution. Emboldened by this success, we apply the

E-mail address: ckchua@phys.ntu.edu.tw (C.-K. Chua).

approach to the charmless modes  $B^0 \rightarrow \rho^- p \bar{n}$ ,  $\pi^- p \bar{n}$  where one replaces the  $D^{*-}$  by  $\rho$  or  $\pi$ .

Besides rates, we are able to predict the  $p \bar{n}$  pair mass spectrum. Since the vector current contributes dominantly to the total rate for the  $B^0 \rightarrow D^{*-} p \bar{n}$  case [7], we expect the vector current to dominate the  $B^0 \rightarrow \rho^- p \bar{n}$  and  $\pi^- p \bar{n}$  rates as well. Incorporating estimates of the axial current contributions, the total rates are slightly higher than from the vector current alone.

## 2. Formalism

Our starting point is to factorize the current production of  $p \bar{n}$  pairs, i.e.,

$$\begin{aligned} & \langle \rho^- (\pi^-) p \bar{n} | \mathcal{H}_{\text{eff}} | B^0 \rangle \\ &= \frac{G_F}{\sqrt{2}} V_{ud} V_{ub}^* a_1 \\ & \times \langle \rho^- (\pi^-) | V^\mu - A^\mu | B^0 \rangle \langle p \bar{n} | V_\mu - A_\mu | 0 \rangle. \end{aligned} \quad (1)$$

The  $V - A$  current induces the  $\bar{b} \rightarrow \bar{u}$  transition in the first term, while in the second it creates the nucleon pair, which is illustrated in Fig. 1. It is an extension of the usual factorization of current–current matrix elements in the case of  $B$  decays to two mesons [12, 13].

Once factorized, the matrix element  $\langle p \bar{n} | V_\mu - A_\mu | 0 \rangle$  describes nucleon pair creation by a charged weak current. The matrix element for the vector ( $V_\mu^+$ ) portion can be expressed as

$$\begin{aligned} & \langle p \bar{n} | V_\mu^+ | 0 \rangle \\ &= \bar{u}(p_p) \left\{ F_1^W(t) \gamma_\mu + i \frac{F_2^W(t)}{2m_N} \sigma_{\mu\nu} q^\nu \right\} v(p_{\bar{n}}), \end{aligned} \quad (2)$$

where  $m_N$  is the nucleon mass,  $q \equiv (p_p + p_{\bar{n}})$  the momentum transfer,  $t \equiv q^2 = m_{p\bar{n}}^2$  the  $p\text{--}\bar{n}$  invariant

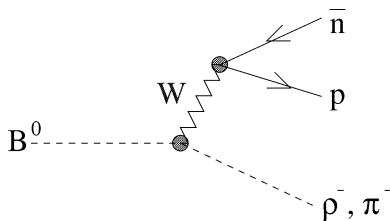


Fig. 1. Feynman diagram illustrating Eq. (1).

mass squared, and  $F_{1,2}^W$  are nucleon weak form factors, with  $F_1^W(t)$  normalized at  $t = 0$  [14],

$$F_1^W(0) = 1. \quad (3)$$

The photon field  $A_\mu$  contains  $W_\mu^3$ , which, together with  $W_\mu^{1,2}$ , form a weak isotriplet. The coupled currents also form an isotriplet, and can be interrelated via an isospin transformation. For the nucleon pair, the strong isospin symmetry of the nucleon state coincides with the weak isospin symmetry of the weak and em currents. The weak vector form factors are therefore related to electromagnetic (em) isovector form factors.

The matrix element  $\langle N(p') \bar{N}(p) | \mathcal{J}_\mu^{\text{em}} | 0 \rangle$  for the em current can be expressed as

$$\begin{aligned} & \langle N(p') \bar{N}(p) | \mathcal{J}_\mu^{\text{em}} | 0 \rangle \\ &= \bar{u}(p') \left\{ F_1(t) \gamma_\mu + i \frac{F_2(t)}{2m_N} \sigma_{\mu\nu} q^\nu \right\} v(p), \end{aligned} \quad (4)$$

where  $F_{1,2}(t)$  are, respectively, the Dirac and Pauli form factors, normalized at  $t = 0$  as

$$\begin{aligned} F_1^p(0) &= 1, & F_1^n(0) &= 0, & F_2^p(0) &= \kappa_p, \\ F_2^n(0) &= \kappa_n, \end{aligned} \quad (5)$$

with  $\kappa_{p(n)}$  the proton (neutron) anomalous magnetic moment in nuclear magneton units. These form factors are related to the Sachs form factors via

$$\begin{aligned} G_E^{p,n}(t) &= F_1^{p,n}(t) + \frac{t}{4m_N^2} F_2^{p,n}(t), \\ G_M^{p,n}(t) &= F_1^{p,n}(t) + F_2^{p,n}(t). \end{aligned} \quad (6)$$

The isospin decomposition of the em current is given by

$$F_i^{s,v} = \frac{1}{2} (F_i^p \pm F_i^n), \quad i = 1, 2, \quad (7)$$

where  $s, v$  stand for the isoscalar and isovector components, respectively. The isovector component of the em current and the vector portion of the charged weak currents form an isotriplet, as manifested by [14]

$$2F_i^v(t) = F_i^W(t), \quad i = 1, 2, \quad (8)$$

where the factor 2 is from the definition of  $F_{1,2}^{(s,v)}(t)$  in Eq. (7). For example, from Eqs. (3), (5) and (7) one easily checks that  $2F_1^v(0) = F_1^W(0)$ .

We can now write the three-body  $B^0 \rightarrow \rho^- p \bar{n}$  decay amplitude in the following form

$$\begin{aligned}
 i\mathcal{M}_V = & \left( -i \frac{G_F}{\sqrt{2}} V_{ud} V_{ub}^* a_1 \right) \\
 & \times \epsilon_\rho^{*v} \left[ -\epsilon_{\mu\nu\alpha\beta} p_B^\alpha p_\rho^\beta \frac{2V(q^2)}{m_B + m_\rho} \right. \\
 & - i g_{\mu\nu} (m_B + m_\rho) A_1(q^2) \\
 & \left. + i (p_B + p_\rho)_\mu q_\nu \frac{A_2(q^2)}{m_B + m_\rho} \right] \\
 & \times \bar{u}(p_p) \left[ 2(F_1^v + F_2^v) \gamma^\mu + \frac{F_2^v}{m_N} (p_{\bar{n}} - p_p)^\mu \right] \\
 & \times v(p_{\bar{n}}), \quad (9)
 \end{aligned}$$

and for  $B^0 \rightarrow \pi^- p \bar{n}$ ,

$$\begin{aligned}
 i\mathcal{M}_P = & \left( -i \frac{G_F}{\sqrt{2}} V_{ud} V_{ub}^* a_1 \right) (p_B + p_\pi)_\mu F_1(q^2) \\
 & \times \bar{u}(p_p) \left[ 2(F_1^v + F_2^v) \gamma^\mu + \frac{F_2^v}{m_N} (p_{\bar{n}} - p_p)^\mu \right] \\
 & \times v(p_{\bar{n}}), \quad (10)
 \end{aligned}$$

where  $\epsilon_\rho$  is the  $\rho$  meson polarization, and  $V(q^2)$ ,  $A_1(q^2)$ ,  $A_2(q^2)$  and  $F_1(q^2)$  (not to be confused with baryon form factors) are the transition form factors arising from the  $\bar{b} \rightarrow \bar{u}$  transition in the first matrix element of Eq. (1).

As we need to integrate over  $q^2$  for these three-body decay modes, we need to pay more attention to the  $q^2$  dependence of these transition form factors [15]. However, since our focus is on utilizing experimental data on baryon form factors, for  $B \rightarrow \rho, \pi$  form factors, we shall simply take what is readily available in the literature. Among the several recent models for the meson form factors (see, e.g., Ref. [16, 17]), we shall use [17]

$$f(q^2) = \frac{f(0)}{(1 - q^2/M_V^2)(1 - \sigma_1 q^2/M_V^2)}, \quad (11)$$

for  $F_1(q^2)$  and  $V(q^2)$ , and

$$f(q^2) = \frac{f(0)}{1 - \sigma_1 q^2/M_V^2 + \sigma_2 q^4/M_V^4}, \quad (12)$$

for  $A_{1,2}(q^2)$ .  $M_V$  is the appropriate pole mass which is taken to be 5.32 GeV. Note that the  $q^2$  dependence is quite different from the monopole form used in Ref. [12]. In Table 1 we give the values of the relevant

Table 1

Form factors at  $q^2 = 0$  and the parameters  $\sigma_{1,2}$

	$V^{B\rho}$	$A_1^{B\rho}$	$A_2^{B\rho}$	$F_1^{B\pi}$
$f(0)$	0.31	0.26	0.24	0.29
$\sigma_1$	0.59	0.73	1.40	0.48
$\sigma_2$	–	0.10	0.50	–

form factors at zero momentum transfer as well as the parameters  $\sigma_{1,2}$  [17].

It is important to note that the baryon form factors must satisfy perturbative QCD (PQCD) quark counting rules [18], which give the leading power large- $|t|$  fall-off of the  $F_1^v(t)$  form factor. Since helicity-flip gives an extra  $1/t$  factor for  $F_2^v(t)$ , one finds in the large  $|t|$  limit

$$F_i^v(t) \rightarrow (|t|)^{-(i+1)} \left[ \ln\left(\frac{|t|}{Q_0^2}\right) \right]^{-\gamma}, \quad i = 1, 2, \quad (13)$$

where  $Q_0 \simeq \Lambda_{\text{QCD}} = 0.3$  GeV,  $\gamma = 2 + 4/(3\beta)$ , and  $\beta$  is the QCD  $\beta$ -function to one loop. We note that  $\gamma$  depends weakly on the number of flavors; for three flavors  $\gamma = 2.148$ . The asymptotic form given in Eq. (13) has been confirmed by many measurements of the nucleon form factors  $G_M^{p,n} = F_1^{p,n} + F_2^{p,n}$  over a wide range of momentum transfers in the space-like region [19]. It has also been confirmed in the time-like region with the recent nucleon time-like data [9–11].

The combination  $2(F_1^v + F_2^v)$  in Eq. (9) can be replaced by  $G_M^p - G_M^n$  which is composed of measurable quantities. Similar replacement can also be made for  $F_2^v$ , which is a combination of  $G_M^p - G_E^p$  and  $G_M^n - G_E^n$ . Most time-like data for the magnetic form factors, however, are extracted by assuming either  $|G_E^N| = |G_M^N|$  or  $|G_E^N| = 0$  in the explored region of momentum transfer. Since  $G_M^N - G_E^N = (1 - t/4m_N^2) F_2^N$  clearly vanishes at threshold, by assuming  $|G_E^N| = |G_M^N|$  in extracting  $G_M^N$  from data, the information on  $F_2^N$  is lost. In our calculation we concentrate on the part of Eq. (9) which contains  $F_1^v + F_2^v$ , the contribution from  $F_2^v$  can be determined only when  $G_M^N$  and  $G_E^N$  can be separated from data with better angular resolution.

We take  $|G_M^N|$  in the following form [7] to make a phenomenological fit of the experimental data [8–11]:

$$|G_M^p(t)| = \sum_{i=1}^5 \frac{x_i}{t^{i+1}} \left[ \ln\left(\frac{t}{Q_0^2}\right) \right]^{-\gamma}, \quad (14)$$

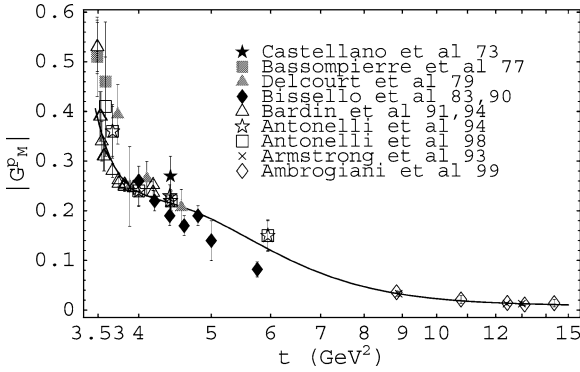


Fig. 2. Time-like proton magnetic form factor data, fitted by Eq. (14) with the parameters given in Eq. (16).

$$|G_M^n(t)| = \sum_{i=1}^2 \frac{y_i}{t^{i+1}} \left[ \ln\left(\frac{t}{Q_0^2}\right) \right]^{-\gamma}, \quad (15)$$

the power of the leading term and logarithmic factor are as suggested by PQCD, and the fewer number of fit parameters for  $G_M^n$  reflects the fact of scarcer neutron data. We find the best fit values

$$\begin{aligned} x_1 &= 429.88 \text{ GeV}^4, & x_4 &= -448583.96 \text{ GeV}^{10}, \\ x_2 &= -10783.69 \text{ GeV}^6, & x_5 &= 635695.29 \text{ GeV}^{12}, \\ x_3 &= 109738.41 \text{ GeV}^8, \end{aligned} \quad (16)$$

and

$$y_1 = 236.69 \text{ GeV}^4, \quad y_2 = -579.51 \text{ GeV}^6, \quad (17)$$

where the  $\chi^2$  per degree of freedom (d.o.f.) of the fits are 1.39 for  $|G_M^p|$  and 0.41 for  $|G_M^n|$ , respectively. We show in Figs. 2 and 3 the best fit curves given by Eqs. (14) and (15) with the above parameters.

It was pointed out in Ref. [10] that the data supports  $|G_E^n| = 0$  as well. We therefore perform a fit to the neutron magnetic form factor data extracted under the assumption of  $|G_E^n| = 0$ , giving the best fit values

$$y_1 = 292.62 \text{ GeV}^4, \quad y_2 = -735.73 \text{ GeV}^6, \quad (18)$$

with  $\chi^2/\text{d.o.f.} = 0.39$ , which is slightly lower than the previous fit. This fit is also plotted in Fig. 3. More data is needed to distinguish between the two cases.

We note that there is a sign difference between  $G_M^p$  and  $G_M^n$  in the space-like region. Since analyticity implies continuity at infinity between space-like and time-like [20] regions, the time-like magnetic form factors are expected to have similar behavior as the

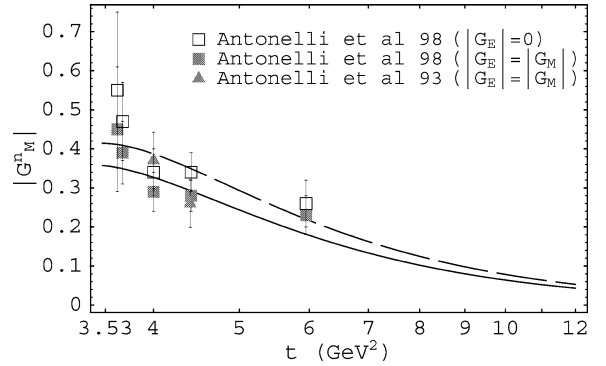


Fig. 3. Time-like neutron magnetic form factor, where the solid (long-dash) line is the fit given by Eq. (15) with parameters given in Eq. (17) (Eq. (18)), for data extracted with  $|G_E^n| = |G_M^n|$  ( $|G_E^n| = 0$ ) assumption.

space-like ones: real and positive for the proton, but negative for the neutron.

For large  $t$ , QCD predicts the magnetic form factors to be real [18], with the neutron form factor weaker than the proton case [21]. According to QCD sum rules [22], asymptotically one expects  $G_M^n/G_M^p \sim Q_d/Q_u = -0.5$ . In our fits, with sign difference between  $G_M^p$  and  $G_M^n$ , we have  $G_M^n/G_M^p = -y_1/x_1 = -0.55$  ( $-0.68$ ) for  $|G_E| = |G_M|$  ( $|G_E^n| = 0$ ). Nucleon form factors have also been analyzed from negative to positive  $t$  with dispersion relations. The phase of the proton magnetic form factor turns out to be  $\sim 2\pi$ , hence the proton magnetic form factor is real and positive as expected asymptotically, starting already from  $t \geq 4 \text{ GeV}^2$  [23,24] onwards.

### 3. Results and discussion

We still need to fix  $V_{ud}V_{ub}^*a_1$ . We shall take  $|V_{ud}| = 0.9747$  and  $|V_{ub}| = 34.95 \times 10^{-4}$  from Ref. [25]. For the effective coefficient  $a_1$ , we take the value  $a_1 = 1.05$  from Ref. [13] for effective number of color  $N_c = 3$ . The situation is slightly different from previous study on  $B^0 \rightarrow D^{*-} p \bar{n}$  case [7], where  $a_1$  is taken from  $B^0 \rightarrow D^{*-} \rho^+$  decay [15]. Here, when one tries to follow the procedure by looking at  $B^0 \rightarrow \rho^- \rho^+$ ,  $\pi^- \rho^+$  modes, the tree-penguin interference will complicate things [1,26]. We therefore use the short distance  $a_1$  for simplicity.

For proton and neutron data extracted assuming  $|G_E^{p,n}| = |G_M^{p,n}|$ , we find the branching ratio for  $B^0 \rightarrow \rho^- p \bar{n}$  arising from the vector current is

$$\text{Br}_V(B^0 \rightarrow \rho^- p \bar{n}) = (3.58_{-0.61}^{+0.70}) \times 10^{-6} \left( \frac{a_1}{1.05} \right)^2, \quad (19)$$

where the subscript  $V$  is a reminder that this is from the vector portion of the weak current alone. The upper and lower bounds correspond, respectively, to the maximum and minimum of the branching fraction evaluated by scanning through  $\chi^2 \leq \chi_{\min}^2 + 1$  in the fits. In a similar fashion, for data extracted assuming  $|G_E^p| = |G_M^p|$  but  $|G_E^n| = 0$ , we find

$$\text{Br}_V(B^0 \rightarrow \rho^- p \bar{n}) = (4.53_{-0.88}^{+1.03}) \times 10^{-6} \left( \frac{a_1}{1.05} \right)^2. \quad (20)$$

Following the same methods, we also give predictions on the  $B^0 \rightarrow \pi^- p \bar{n}$  rate that arise from the vector current. We find

$$\text{Br}_V(B^0 \rightarrow \pi^- p \bar{n}) = (1.82_{-0.16}^{+0.17}) \times 10^{-6} \left( \frac{a_1}{1.05} \right)^2, \quad (21)$$

for  $|G_M^{p,n}| = |G_E^{p,n}|$ , and

$$\text{Br}_V(B^0 \rightarrow \pi^- p \bar{n}) = (2.29_{-0.42}^{+0.49}) \times 10^{-6} \left( \frac{a_1}{1.05} \right)^2, \quad (22)$$

for  $|G_E^p| = |G_M^p|$  but  $|G_E^n| = 0$ .

Fig. 4 shows the vector current induced differential decay rates  $d\Gamma_V/dq^2$  of both the  $B^0 \rightarrow \rho^- p \bar{n}$  and the  $\pi^- p \bar{n}$  modes with BSW form factors. The peaking of the differential rates at  $\sim 5 \text{ GeV}^2$  and  $\sim 4 \text{ GeV}^2$  for the  $\rho^- p \bar{n}$  and  $\pi^- p \bar{n}$  modes, respectively, is a threshold enhancement effect for baryon production. As argued in [2], a fast recoil meson carries away energy and would be more favorable for baryon production in the recoil system because of reduced energy release compared to two-body decays. This fast recoil meson accompanying the low mass baryon pair can be tested experimentally. We note that the narrowness of the  $t$  distribution in Fig. 4 implies the recoil meson spectrum of a quasi-two-body mode.

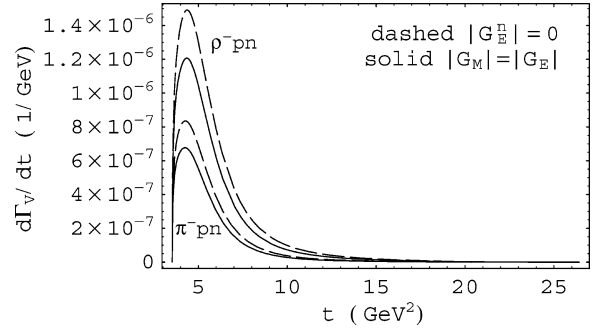


Fig. 4. The vector current induced differential decay rates  $d\Gamma_V(B^0 \rightarrow \rho^- p \bar{n})/dq^2$  (upper two curves) and  $d\Gamma_V(B^0 \rightarrow \pi^- p \bar{n})/dq^2$  (lower two curves). Solid lines are from fitting nucleon form factor data with  $|G_M^{p,n}| = |G_E^{p,n}|$ , dashed lines with  $|G_M^p| = |G_E^p|$  and  $|G_E^n| = 0$ .

According to the  $B^0 \rightarrow D^{*-} p \bar{n}$  study [7], the vector current contributes  $\sim 60\%$  of the observed rate [5]. We can estimate the total rates of the  $B^0 \rightarrow \rho^- p \bar{n}$ ,  $\pi^- p \bar{n}$  modes by assuming similar proportions of the vector current contributions. The estimated rates are then  $\text{Br}(B^0 \rightarrow \rho^- p \bar{n}) \sim 7 \times 10^{-6}$  and  $\text{Br}(\pi^- p \bar{n}) \sim 3 \times 10^{-6}$ , i.e.,  $B^0 \rightarrow \rho^- p \bar{n}$  is of order  $10^{-5}$ . Inspection of Fig. 1 suggests that  $B^+ \rightarrow \rho^0 p \bar{n}$  is at the same order.

It is interesting to compare the three-body rates  $\text{Br}(B^0 \rightarrow h p \bar{n})$  with the two-body ones  $\text{Br}(B^0 \rightarrow h \rho^+)$  where  $h$  stands for the recoil meson. We find a similarity of the ratios  $\text{Br}(3\text{-body})/\text{Br}(2\text{-body})$  between  $h = D^{*-}$  and  $h = \rho^-, \pi^-$ . By taking  $\phi_3 = 54.8^\circ$  [25], we obtain  $\text{Br}(\rho^- \rho^+ (\pi^- \rho^+)) \sim 32 (22) \times 10^{-6}$  [26]. We then have  $\text{Br}(\rho^- p \bar{n} (\pi^- p \bar{n}))/\text{Br}(\rho^- \rho^+ (\pi^- \rho^+)) \sim 0.22 (0.14)$  which is rather close to  $\text{Br}(D^{*-} p \bar{n})/\text{Br}(D^{*-} \rho^+) \sim 0.2$ .

So far, we have assumed only the tree level  $b \rightarrow d \bar{u} u$  transitions as the underlying process, as illustrated in Eq. (1) and Fig. 1. As we make comparison with charmless mesonic modes, it is important to remember that, unlike the  $B^0 \rightarrow D^{*-} p \bar{n}$  case, we expect significant penguin contributions as well. It is known that  $b \rightarrow s \bar{u} u$  penguins dominate  $K\pi$  modes, and that penguin contributions make significant impact on  $\pi\pi$  modes. Since the impact of penguins becomes less pronounced for  $VP$  and  $VV$  modes, and since our approach to  $\rho^- p \bar{n}$  corresponds to both  $VP$  and  $VV$  components, we expect the impact of penguins on  $B^0 \rightarrow \rho^- p \bar{n}$  to be not as pronounced

as in  $B^0 \rightarrow \pi^+\pi^-$ . On the other hand, extending our discussion to  $b \rightarrow s$  penguin operators suggests three-body charmless baryonic modes such as  $\rho^-\Lambda\bar{p}$ ,  $K^*\Lambda\bar{S}$ , etc. However, this would involve further assumptions.

With recent improvement of  $B^0 \rightarrow p\bar{p}$  limit to  $10^{-6}$  level [4], we now have the intriguing situation that  $B \rightarrow \rho p\bar{n} \gg B \rightarrow p\bar{p}$ , i.e., the three-body baryonic mode dominates over the two-body. This would confirm the conjecture made in Ref. [2]. We urge the Belle and BaBar groups to search for the three-body modes experimentally.

In summary, from a relatively robust foundation, in analogy with the  $B^0 \rightarrow D^{*-}p\bar{n}$  mode observed by CLEO, we have shown that  $B^0 \rightarrow \rho^-p\bar{n}$  is very likely at the  $10^{-5}$  level and should be well within the capabilities at  $B$  factories. Together with the absence of two body modes such as  $B^0 \rightarrow p\bar{p}$ , the dynamics of  $B$  decay to baryons are somewhat different from mesonic final states. Extending our study to include the standard set of effective operators should be straightforward, and one expects a host of three-body baryonic modes at the  $10^{-5}$  level. We expect charmless baryonic modes to emerge soon at the  $B$  factories, likely from three-body onwards.

## Acknowledgements

This work is supported in part by the National Science Council of R.O.C. under Grants NSC-89-2112-M-002-063, NSC-89-2811-M-002-0086 and NSC-89-2112-M-002-062, the MOE CosPA project, and the BCP topical program of NCTS.

## References

- [1] X.-G. He, W.-S. Hou, K.-C. Yang, Phys. Rev. Lett. 83 (1999) 1100, hep-ph/9902256.
- [2] W.-S. Hou, A. Soni, Phys. Rev. Lett. 86 (2001) 4247, hep-ph/0008079.
- [3] T.E. Coan et al., CLEO Collaboration, Phys. Rev. D 59 (1999) 111101, hep-ex/9810043.
- [4] K. Abe et al., Belle Collaboration, BELLE-CONF-0116.
- [5] S. Anderson et al., CLEO Collaboration, Phys. Rev. Lett. 86 (2001) 2732, hep-ex/0009011.
- [6] D.E. Groom et al., Particle Data Group Collaboration, Eur. Phys. J. C 15 (2000) 1.
- [7] C.-K. Chua, W.-S. Hou, S.-Y. Tsai, hep-ph/0107110.
- [8] M. Castellano et al., Nuovo Cimento A 14 (1973) 1; G. Bassompierre et al., Mulhouse–Strasbourg–Turin Collaboration, Phys. Lett. B 68 (1977) 477; B. Delcourt et al., Phys. Lett. B 86 (1979) 395; D. Bisello et al., Nucl. Phys. B 224 (1983) 379; D. Bisello et al., Z. Phys. C 48 (1990) 23; G. Bardin et al., Phys. Lett. B 255 (1991) 149; G. Bardin et al., Phys. Lett. B 257 (1991) 514; G. Bardin et al., Nucl. Phys. B 411 (1994) 3; A. Antonelli et al., Phys. Lett. B 313 (1993) 283; A. Antonelli et al., Phys. Lett. B 334 (1994) 431.
- [9] T.A. Armstrong et al., E760 Collaboration, Phys. Rev. Lett. 70 (1993) 1212.
- [10] A. Antonelli et al., Nucl. Phys. B 517 (1998) 3.
- [11] M. Ambrogiani et al., E835 Collaboration, Phys. Rev. D 60 (1999) 032002.
- [12] M. Wirbel, B. Stech, M. Bauer, Z. Phys. C 29 (1985) 637; M. Bauer, B. Stech, M. Wirbel, Z. Phys. C 34 (1987) 103.
- [13] A. Ali, G. Kramer, C.-D. Lu, Phys. Rev. D 58 (1998) 094009, hep-ph/9804363.
- [14] See, for example, H. Georgi, Weak Interactions and Modern Particle Theory, Benjamin–Cummings, 1984.
- [15] See, for example, H.-Y. Cheng, K.-C. Yang, Phys. Rev. D 59 (1999) 092004, hep-ph/9811249.
- [16] V.M. Braun, hep-ph/9911206.
- [17] D. Melikhov, B. Stech, Phys. Rev. D 62 (2000) 014006, hep-ph/0001113.
- [18] S.J. Brodsky, G.R. Farrar, Phys. Rev. D 11 (1975) 1309.
- [19] T. Jansens et al., Phys. Rev. 142 (1965) 922; W. Bartel et al., Phys. Lett. B 33 (1970) 245; C. Berger et al., Phys. Lett. B 35 (1971) 87; F. Borkowski et al., Nucl. Phys. B 93 (1975) 461; G. Höhler et al., Nucl. Phys. B 114 (1976) 505; R.G. Arnold et al., Phys. Rev. Lett. 57 (1986) 174; R.C. Walker et al., Phys. Lett. B 224 (1989) 353; R.C. Walker et al., Phys. Lett. B 240 (1989) 522, Erratum.
- [20] A.A. Logunov, N. Van Hieu, I.T. Todorov, Ann. Phys. 31 (1965) 203.
- [21] V.A. Matveev, R.M. Muradyan, A.N. Tavkhelidze, Lett. Nuovo Cimento 7 (1973) 719.
- [22] V.L. Chernyak, I.R. Zhitnitsky, Nucl. Phys. B 246 (1984) 52.
- [23] H.-W. Hammer, U.-G. Meissner, D. Drechsel, Phys. Lett. B 385 (1996) 343, hep-ph/9604294.
- [24] R. Baldini et al., Eur. Phys. J. C 11 (1999) 709.
- [25] M. Ciuchini et al., JHEP 0107 (2001) 013, hep-ph/0012308.
- [26] W.-S. Hou, K.-C. Yang, Phys. Rev. D 61 (2000) 073014, hep-ph/9908202.